sciendo

Civil and Environmental Engineering
Vol. 19, Issue 1, 167-177, DOI: 10.2478/cee-2023-0015

PARAMETRIC STUDY OF DRILLING METHOD PERFORMED ON ONE-WAY POST-TENSIONED SLABS

Jakub KRALOVANEC[1,*], Martin MORAVČÍK[2]

[1] GEART, s.r.o., P.O. Hviezdoslava 42A, 010 01 Žilina, Slovakia.
[2] Department of Structures and Bridges, Faculty of Civil Engineering, University of Žilina, Univerzitná 8215/1, 010 26 Žilina, Slovakia.
[*] corresponding author: jakub.kralovanec@uniza.sk

Abstract

Determination of the stress state in concrete structures is a very important, but difficult task. In the case of new structures, it is possible to easily instal measurement instruments which can provide important data as a part of real-time monitoring. However, the evaluation of stresses in existing structures is much more challenging. Currently, stress relief methods are a well-established approach for the evaluation of the actual state of existing structures. The so-called Drilling method (also known as Stress-relief coring technique) is one of the possible techniques for such analysis. For practical use of this method, knowledge of pivotal factors which influence stress relief is crucial. Therefore, this paper presents a parametric study performed on a one-way post-tensioned slab which can help to understand the effect of the depth of the core and the distance from the edge of the hole (position of strain gauges) on the change in stress in the vicinity of the drilled core. Finally, based on the obtained data, the recommendations for the subsequent experimental program will be summarized. According to the study, it seems that the depth of drilled core does not significantly influence the stress relief and the main impact can be attributed to distance from the edge of the hole.

Keywords:

Drilling method;
Stress-relief coring technique;
Indirect methods;
Prestressing;
Parametric study.

1 Introduction

Nowadays, analysis of residual prestressing has become more and more important especially because the current tendency is sustainability with minimal impact on the environment [1, 2]. The reason is the bad state of existing prestressed concrete structures. Furthermore, residual prestressing force value is the crucial factor for the subsequent determination of load-carrying capacity and remaining service life of the assessed structure. Therefore, its determination is a very important, but difficult task [3]. Besides other factors, the rheology of concrete has a significant influence on the overall state of prestressing [4]. The biggest challenges in the evaluation of prestressing force include the absence of drawings or other relevant information about existing structures (bridges) and unknown material properties. However, this information can be obtained in situ, but such a diagnostic survey can be much more expensive than a standard visual inspection. Consequently, the determined residual prestressing force value is subsequently used in advanced analyses. For this reason, we need to know whether it is possible to rely on the obtained parameters. Such an approach can give us a better picture of the state of the prestressed concrete structure. Moreover, some authors also describe the importance of the application of construction error models in order to the definition of partial safety factors and future revisions of design and assessment codes [5]. Therefore, regular inspections and determination of prestressing of existing structures can also help the administrators in decision-making. The performed diagnostic survey should also consider possible settlements which influence the behaviour of structure [6-8].

The actual stresses in concrete structures can be evaluated using two methodologies – installation of measuring instruments into the structure during the construction process (new

structures) or application of several techniques such as stress relief methods (existing structures) [9]. Engineers can apply a lot of available methods for pressing force monitoring. In practice, it is very important to preserve the integrity of the investigated structure. Therefore, the application of non-destructive or semi-destructive techniques is a suitable option. Non-destructive methods affect the assessed member only locally and produced damages which can be easily and properly repaired in a short time. In [10], the authors describe new trends in the field of monitoring residual prestressing force and present dynamic free vibration and ultrasonic tests which can be also a possible option. They also used a suitable combination of stress release methods with X-ray diffractometry. Static and dynamic tests performed to determine the structural response were described, for example, in [11].

So-called stress release methods are one of the possibilities. In the case of beam structures (e.g., girder bridges), we can easily use the Saw-cut method [12]. This method is based on the application of small interventions to assess the beam in form of saw-cuts. This intervention causes the isolation of the concrete block from the acting forces and the normal stress relief is measured in the area adjacent to saw-cuts. This way, we can indirectly calculate the residual prestressing force on the unloaded structure, as only dead load and prestressing in question contribute to normal stress distribution in uncracked cross-section. Unfortunately, this approach is very difficult to apply to prestressed slab structures or on structures which are composed of several slabs, such as prestressed box girder brides. Therefore, we can use other options in for of the so-called Drilling method which is also known as the Stress relief coring technique [13]. The principle of this procedure is very similar to the Saw-cut method, see Fig. 1. The only difference is that the stress relief is caused by drilling, so the stress change is monitored in the vicinity of the relatively small hole which is drilled in a concrete member. Total stress relief (100 %) can be observed at the edge of the hole where radial stress is zero. The stress relief disappears as the distance from the drilled hole increases.

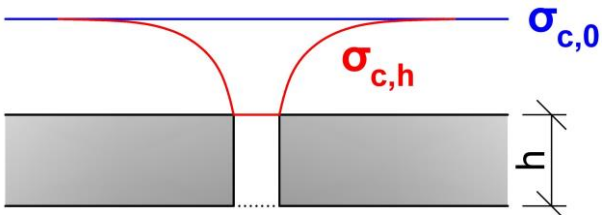

Fig. 1: Principle of drilling method.

The drilling method was originally used in the field of the measurement of metal material components and the first applications are attributed to Mathar in 1934 [14]. Since then, this approach has become standard for the determination of residual stresses in steel structures. In the case of metal materials, the drilled hole is small (diameter only circa 1.5 mm) [15-17]. Therefore, such small holes are not applicable for concrete members (need for longer strain gauges and heterogeneity of concrete) [17]. However, this technique inspired engineers to evaluate concrete structures too. In the past, the Drilling method performed on concrete structures was studied by several authors with various modifications. In [18], the authors suggest measuring the strain change at a distance of about two-hole diameters from the centre of the drilled core. They concluded that concrete stresses should be released by using a diamond drill, which produces a circular hole with a diameter from 77 to 79 mm with depts from 100 to 175 mm. Shallow depths of the core could result in only a partial relief which would affect the accuracy of the performed method. More recent work [19] proposes to produce a hole with a diameter of 50 mm or 100 mm, which is considered a better option. According to [20], the diameters of drilled cores should be 100 mm, 75 mm, or 50 mm, while the depth of the drilling step should be 5 mm. The drilled concrete cores are later used for evaluation of the modulus of elasticity [21]. In [22-24], the researchers combined the drilling method with digital image correlation. Moreover, they have considered the effects of water during drilling, the shrinkage of concrete, and the presence of reinforcement. In 2020, Deng and Tang [15] described a new system of this approach that combines strain gauges with a core-drilling machine to measure the released strain. This way, they managed to solve the problem of borehole strain gauge wiring (the strain gauge is placed inside the core) in case of uniaxially stressed concrete beam which was experimentally and numerically analysed. If we cut the steel reinforcement, it is important to consider its influence. Hence, the identification of the reinforcement in advance is very important, so we can avoid its cutting [15]. In [23], the authors presented an analysis performed on steel members instead of concrete elements. They chose this material to provide a specimen with a known modulus of elasticity, to ensure a fine-grained

(homogenous) specimen, and to perform the test in the case of tensile stresses. This method has the potential for application to structures such as bridges, buildings, dams, retaining walls, tunnels, shafts and so on [23]. Generally, wherever we need to determine the actual stress state.

A modified version of this method was even applied to beam members [25]. The authors analysed 25-year-old prestressed concrete girder with the application of a small cylindrical hole drilled in the bottom flange. This modification requires the determination of side pressure (hoop stress) which is required to close an inducted crack in the vicinity of the drilled hole [26]. Similarly, in [6] the researchers applied this method to longitudinally loaded members (only axial compression) with a length of 500 mm, and a cross-section of 100 x 200 mm.

In the case of the assessment of slab structures 2D, we have to deal with two-dimensional stress distribution. The drilling method involves the measurement of strains along the so-called measurement circle. The strains consist of radial *u* and tangential *v* components. Consequently, any 2D stress distribution can be decomposed into a mean stress component (*P*, also known as equiaxial stress), a deviatoric stress component *Q*, and a shear stress component *τ* [27], see equations (1-3). Parameters of measurement layout include the diameter of drilled core *Φ*, the distance of the measurement circle from the edge of drilled core (d) and the angle between the point on the measurement circle and the x-axis *θ*. These parameters are shown in Fig. 2. More information can be found for example in [22, 24, 27].

$$P(H) = \frac{\sigma_{xx}(H)+\sigma_{yy}(H)}{2}, \tag{1}$$

$$Q(H) = \frac{\sigma_{xx}(H)-\sigma_{yy}(H)}{2}, \tag{2}$$

$$\tau_{xy}(H) = \tau_{xy}(H). \tag{3}$$

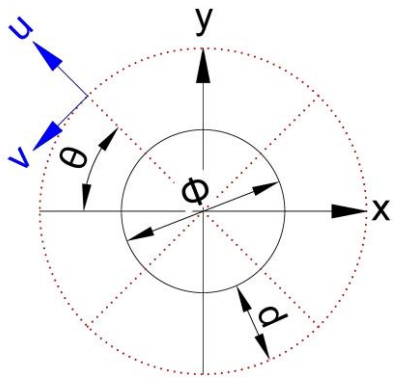

Fig. 2: Measurement circle with its parameters.

2 Numerical analysis

2.1 Specimens

The analysis is performed on the one-way post-tensioned slabs with a length l_x of 2000 mm, a width l_y of 1000 mm and a depth *h* of 200 mm. The prestressing of the slabs is provided by two prestressing bars with a diameter of 20 mm at a distance of 250 mm from the edges. The dimensions and the reinforcement layout of the slab are presented in Fig. 3. The ratio of the longitudinal and transversal l_x/l_y = 2.0. Therefore, the slab in question can be considered one-way (load transfer mainly in the transversal direction). For the analysis, the slabs are supported by two line supports (steel rollers) located 100 mm from the ends. As a result, the specimen acts with the static scheme of a simply supported beam with an effective length of 1800 mm.

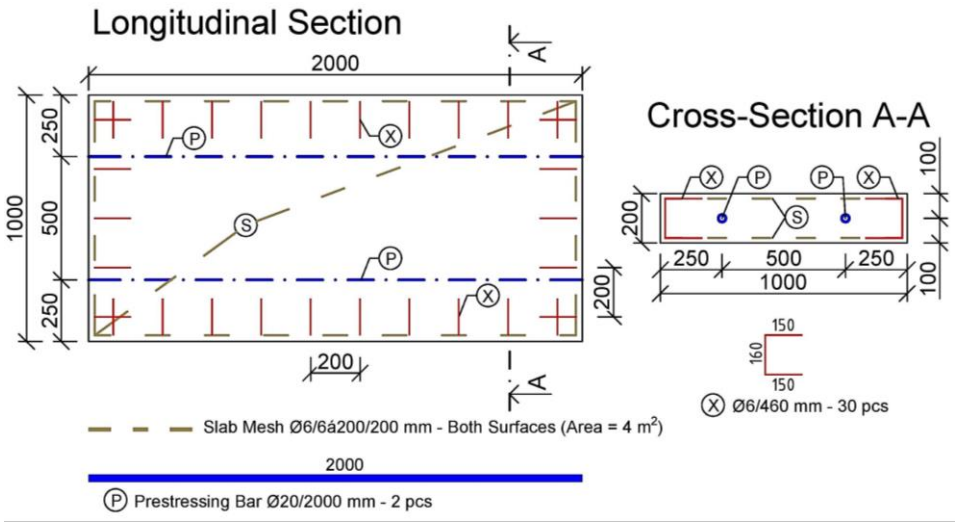

Fig. 3: Dimensions [mm] and reinforcement layout of the analysed slabs.

2.2 Strain gauges arrangement

The aim of the presented analysis is to determine factors which influence stress relief in the above-mentioned slab specimens. Therefore, overall, three different layouts of strain gauges were studied. In this study, strain gauges with a measuring grid length of 100 mm are used. First, the middle of the strain gauges arrangement is located at the distance of one diameter 1.0Φ = 100 mm from the edge of the drilled core with the standard diameter of 100 mm. Second, the strain gauges are placed at a distance of one and a half diameters 1.5Φ = 150 mm from the drilled hole. Finally, the centre of the strain gauges is two diameters 2.0Φ = 200 mm from the edge of the core. In the numerical analysis, eight strain gauges are used. Two of them are monitoring stress $\sigma_{c,xx}$ and two $\sigma_{c,yy}$. Moreover, four strain gauges observe stress changes deflected by θ = 45° ($\sigma_{c,45°}$). The strain gauges layout can be seen in Fig. 4.

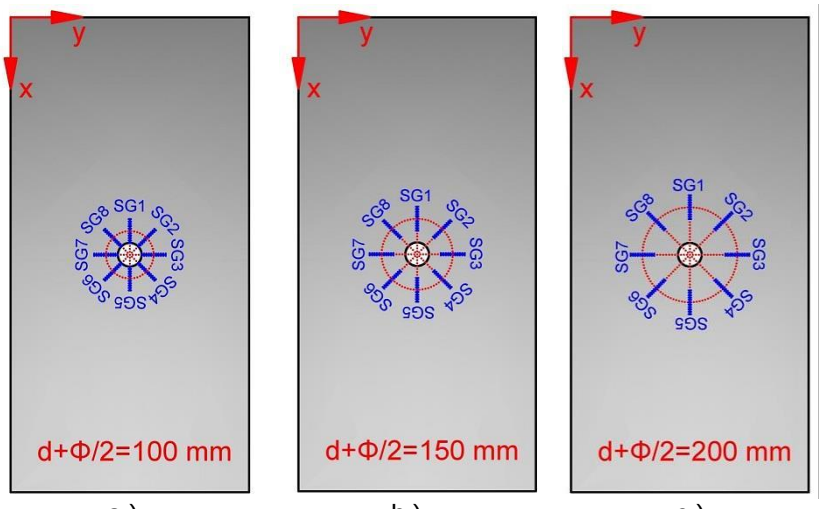

a.) b.) c.)

Fig. 4: Three analysed strain gauges arrangement – a.) 1.0Φ; b.) 1.5Φ; c.) 2.0Φ.

2.3 Numerical model

A nonlinear numerical model was created in the ATENA 3D Software (version ATENA 5.7.0n, Červenka Consulting, Prague, Czech Republic) [28-30]. The analysed specimen in form of a one-way post-tensioned slab was modelled to simulate the change in stress during the gradual application of the Drilling method. Model in ATENA 3D Software is shown in Fig. 5. Stress relief was monitored in the vicinity of the drilled core with a diameter of 100 mm which is located in the middle of the specimen (x = 1000 mm; y = 500 mm). Considering the real position of steel rollers, the line supports were modelled at a distance of 100 mm from the edge of the slab (the effective span of the simply

supported beam was 1800 mm). The prestressing bars were assigned as discrete 1D (truss) elements.

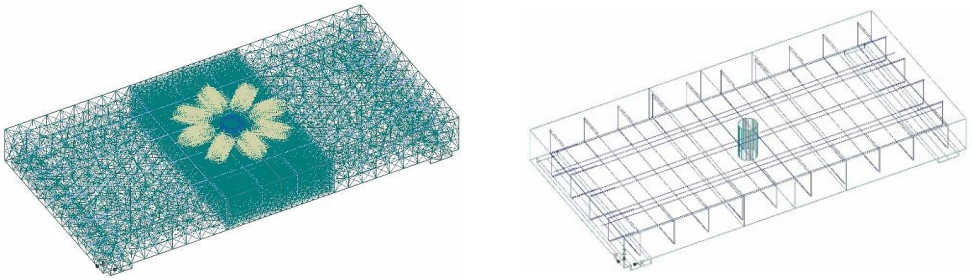

a) b)

Fig. 5: FEM model in ATENA 3D Software – a) FE mesh and monitoring points; b) reinforcement.

Material parameters of concrete were assigned according to the results of material properties testing, which was part of the experiment program. However, detailed material properties that could not be defined during testing were specified according to the recommendations which are presented in [26]. The concrete specimen was simulated by material type “3D Nonlinear Cementitious 2”. It is well known that the size of finite element mesh has a huge impact on the obtained results. Usually, it is advised to model members with at least 4 to 6 elements per thickness of macro-element. In this case, all modelled elements were assigned as a tetrahedral element CCIso Tetra, which the detailed mathematical description containing interpolation functions is given in [28]. The geometry of these elements is displayed in Fig. 6. The global size of the slab's elements was 80 mm. The central area of the specimen was refined into tetrahedral elements with a size of 30 mm, whereas the mesh of the drilled core was smoothed into 20 mm elements. The mesh generation was performed using an automatic mesh generator which is implemented in the ATENA 3D Software.

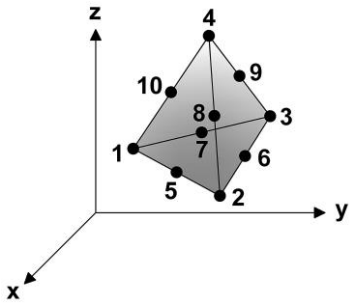

Fig. 6: Tetrahedral element CCIso Tetra.

According to [26], the fracture-plastic model 3D Nonlinear Cementitious 2 describes constitutive models for tensile (fracturing) and compressive (plastic behaviour). The fracture model of the numerical simulation is based on the classical orthotropic smeared crack formulation and crack band model. In the analysis, the Rankine failure criterion and exponential softening are employed. Moreover, it can be used as a rotated or fixed crack model. The hardening and softening plasticity model are based on the so-called Menétrey-Willam failure surface, and this model operates a return mapping algorithm for the integration of constitutive equations. The implemented algorithm allows the combination of two models. Consequently, two models can be developed and formulated separately. Strain decomposition into elastic, plastic, and fracturing components is the basis for the formulation of the material model. Fracture-Plastic Constitutive Model is detailed described in [28]. Stress-strain curves for concrete are shown in Fig. 7. In the performed numerical analysis, the assumption of elastic-perfectly plastic (bilinear law) was employed.

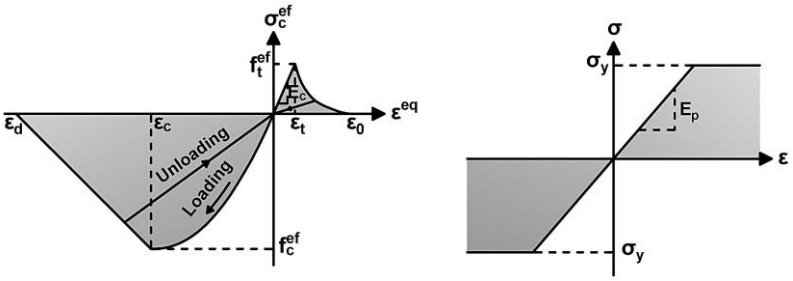

a) b)

Fig. 7: a) Uniaxial stress–strain curve for concrete; b) Stress–strain curve for prestressing bars.

Analysis performed in ATENA 3D Software was based on the Newton-Raphson method. In detail, the method keeps the load increment unchanged and iterates displacements until equilibrium is satisfied within the given tolerance. Hence, this method should be used when load values have to be exactly met and are used in the case of loads including body forces, temperature, shrinkage, and prestressing. In the case of the presented numerical analysis, overall, three loading cases were modelled (support, self-weight and prestressing). The gradual drilling was simulated using so-called construction stages. Every stage represents an increment of 50 mm until the whole slab is drilled (the maximum depth of drilled core was 200 mm. Finally, stress relief was monitored after every stage. The view on the individual stages 0 - 4 is presented in Fig. 8.

a) b) c) d) e)

Fig. 8: a) Stage 0: h = 0 mm; b) Stage 1: h = 50 mm; c) Stage 2: h = 100 mm; d) Stage 3: h = 150 mm; e) Stage 4: h = 200 mm.

In the numerical model, the strain gauges were represented by the group of eleven monitoring points along the assumed measuring grid length 100 mm. Consequently, these monitoring points were distanced from each other by 10 mm. Overall stress change was considered as an average value from these eleven monitoring points.

2.4 Results from numerical analysis

The aim of the performed analysis is the observation of the development of stress relief on the top surface of a one-way simply supported post-tensioned slab during gradual drilling. Stresses $\sigma_{c,xx}$ and $\sigma_{c,yy}$ in each stage are presented in Fig. 9-13. The stresses $\sigma_{c,45°}$ in deflected strain gauges θ = 45° were determined using the transformation of obtained stresses in the x and y directions.

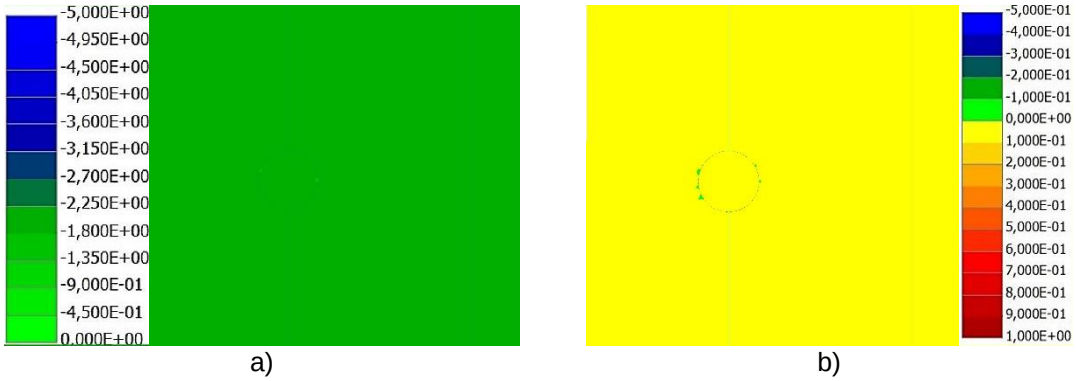

a) b)

Fig. 9: Stress contour areas [MPa] – Stage 0 (h = 0 mm), a) $\sigma_{c,xx}$; b) $\sigma_{c,yy}$.

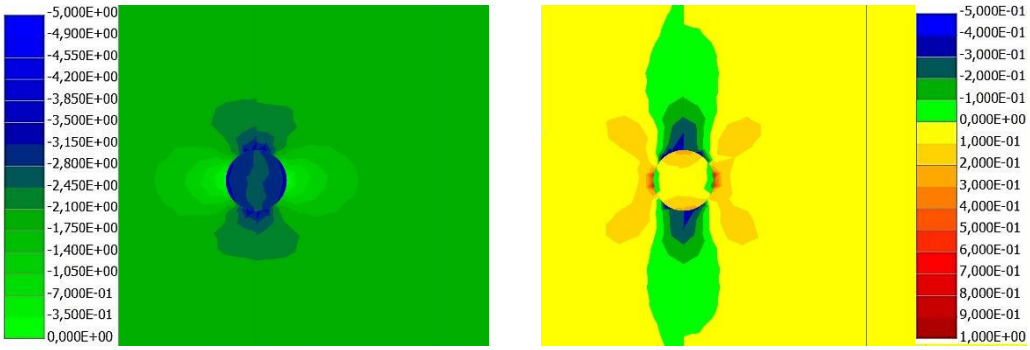

a) b)

Fig. 10: Stress contour areas [MPa] – Stage 1 (h = 50 mm), a) $\sigma_{c,xx}$; b) $\sigma_{c,yy}$.

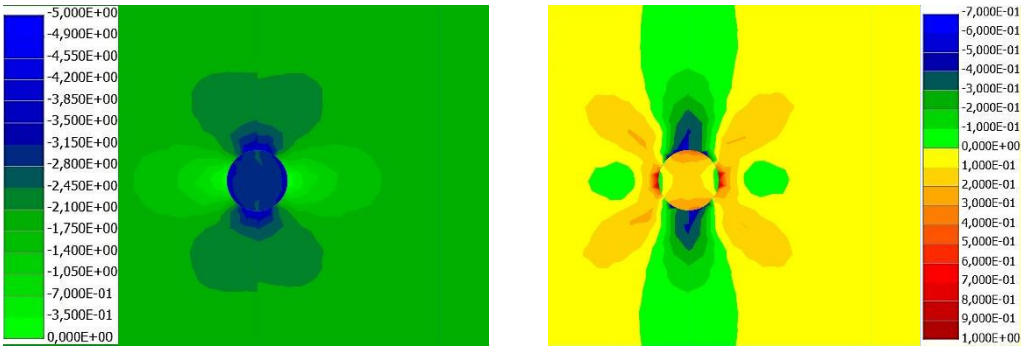

a) b)

Fig. 11: Stress contour areas [MPa] – Stage 2 (h = 100 mm), a) $\sigma_{c,xx}$; b) $\sigma_{c,yy}$.

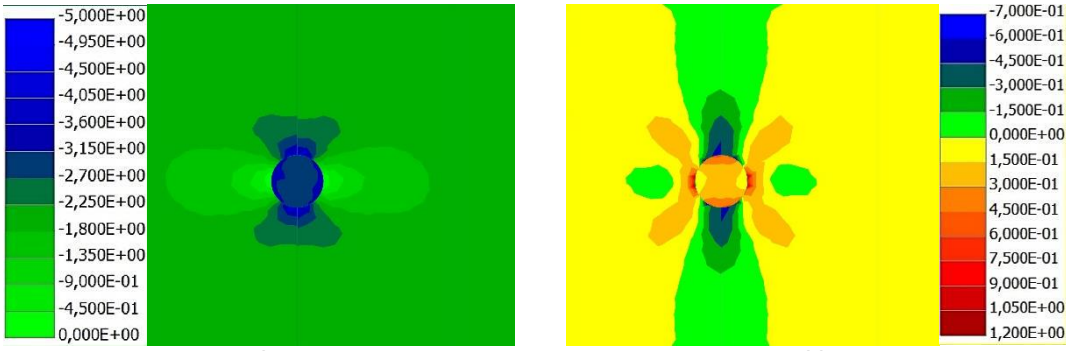

a) b)

Fig. 12: Stress contour areas [MPa] – Stage 3 (h = 150 mm), a) $\sigma_{c,xx}$; b) $\sigma_{c,yy}$.

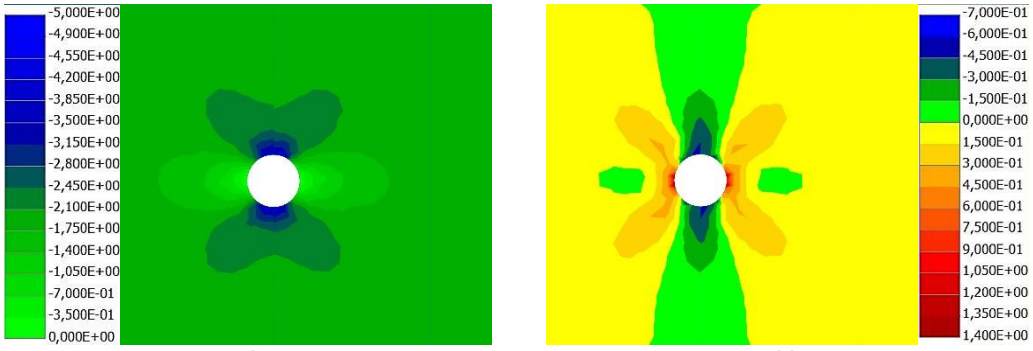

a) b)

Fig. 13: Stress contour areas [MPa] – Stage 4 (h = 200 mm), a) $\sigma_{c,xx}$; b) $\sigma_{c,yy}$.

3 Parametric study

For a better understanding of the influence of drilled core parameters, several depths and distances from the edge of the hole were studied. Regarding the depth of the core, four increments

were considered – 50 mm; 100 mm; 150 mm, and 200 mm (0.25*h*; 0.50*h*; 0.75*h*; and 1.0*h*). In the case of the impact of the distance from the drilled core, a 200 mm long area was studied (this length represents the two-time diameter of the core). Fig. 14 depicts the stress $\sigma_{c,xx}$ from the edge of the drilled hole up to point in a distance of 200 mm. Obviously, full stress relief can be observed on the edge of the core and the stress reaches the initial value with increasing distance. For instance, the change in stress at a distance of 100 mm from the edge of the drilled core is very small only 10 - 20 %. Fig. 15 displays the change in stress $\sigma_{c,xx}$ in relation to the distance from the core's edge.

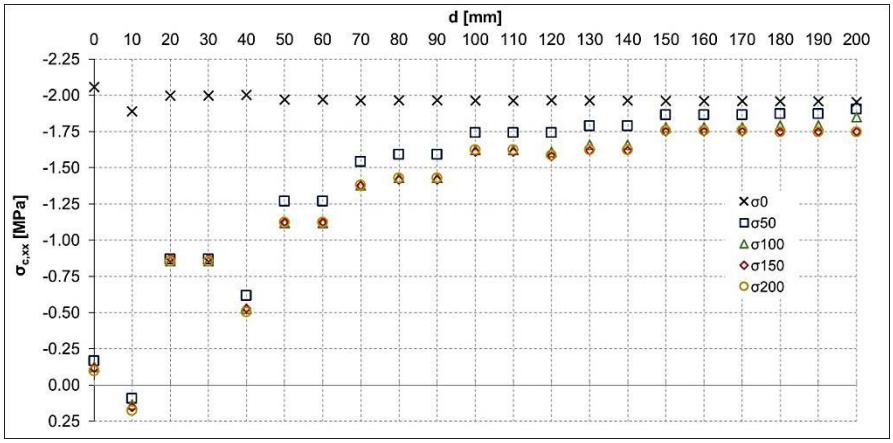

Fig. 14: Relationship between stress $\sigma_{c,xx}$ and distance *d* from the edge of the drilled core.

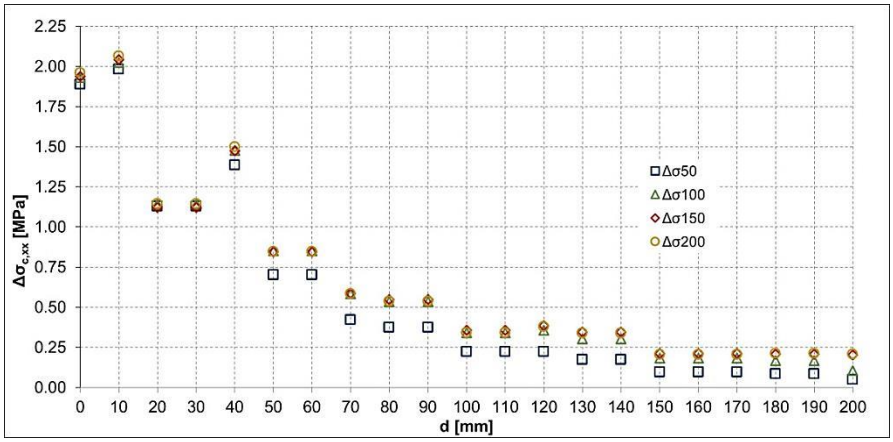

Fig. 15: Relationship between stress change $\Delta\sigma_{c,xx}$ and distance *d* from the edge of the drilled core.

Since, the analysed specimen is a one-way slab, the stress $\sigma_{c,yy}$ is negligible in comparison to stress $\Delta\sigma_{c,xx}$. Therefore, the measurement of the stress change using linear foil strain gauges would be very complicated, see Fig. 16.

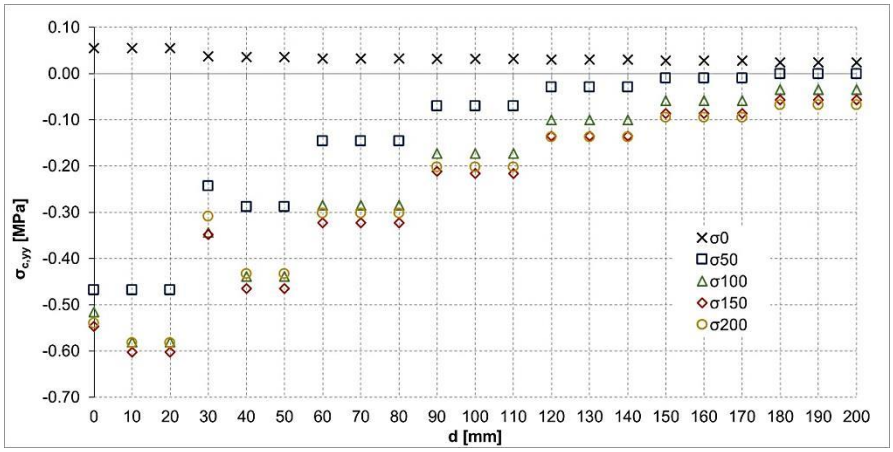

Fig. 16: Relationship between stress $\sigma_{c,yy}$ and distance *d* from the edge of the drilled core.

Similar to stress $\sigma_{c,yy}$, stresses deflected by 45° ($\sigma_{c,45°}$) are not a very good option in the case of a one-way slab. Moreover, the results are not consistent, and the evaluation would be very complicated in the experimental program. The relation between stress $\sigma_{c,45°}$ and distance from the edge of the drilled core can be seen in Fig. 17.

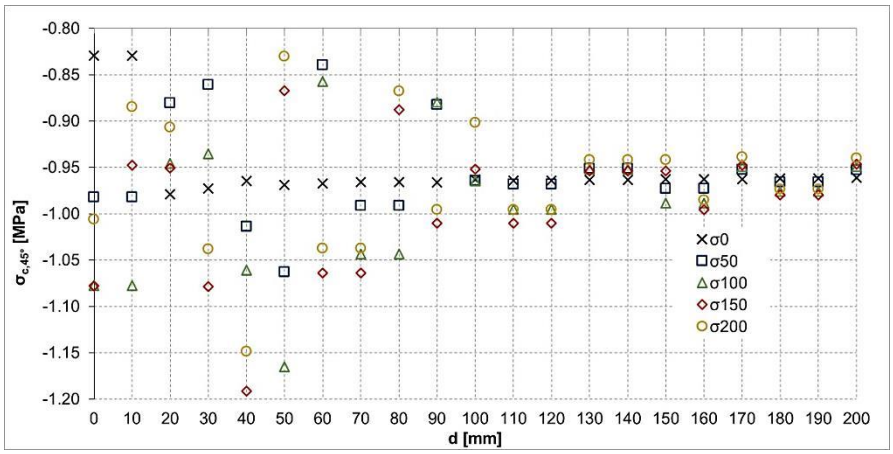

Fig. 17: Relationship between stress $\sigma_{c,45°}$ and distance d from the edge of the drilled core.

As a result of performed numerical analysis, only the measurement of stress $\sigma_{c,xx}$ seems to be applicable in the experimental program. Finally, the regression analysis was performed to describe the relationship between the stress relief and the distance of the monitoring point from the drilled core's edges. Fig. 18 presents the result of the regression analysis which is based on the outputs of numerical simulation in ATENA 3D Software.

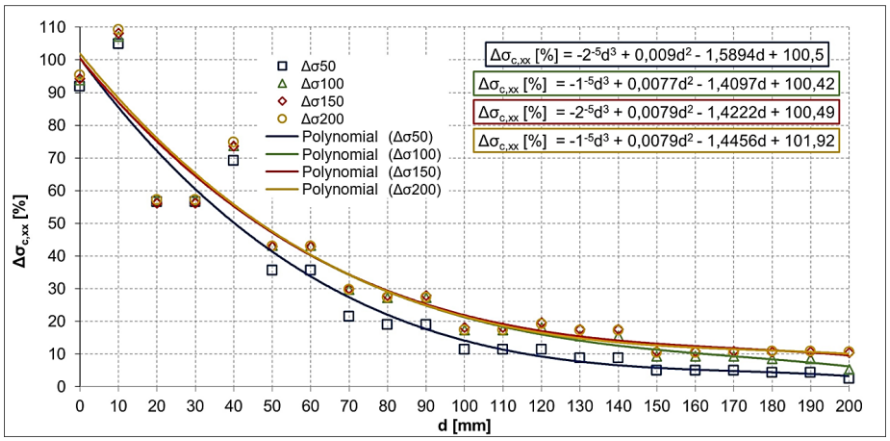

Fig. 18: Relationship between percentage stress change $\Delta\sigma_{c,xx}$ and distance d from the edge of the drilled core.

4 Conclusions

The conclusions from the numerical analysis and subsequent regression analysis performed on a one-way post-tensioned slab can be summarized as follows:

1) The deeper the drilled core is, the more stress is released from the surface. However, the differences in the case of the drilled core with a depth of a quarter of the thickness of the slab and more are very small. Consequently, if the situation does not allow drilling through the entire slabs, it seems sufficient to proceed only to partial drilling of the core.

2) Notable stress relief can be observed up to the distance of approximately one diameter Φ = 100 mm of the core from the edge of the drilled hole. As a result, the strain gauges should be installed as close as it is possible in the vicinity of the core to ensure a sufficient change in stress. In the case of the strain gauges with a measuring grid of 100 mm, the position of the centre of the measuring grid of 1.5 times the diameter of the drilled hole seems to be sufficient. If the quality of the surface and the size of the aggregate allow it, the strain gauges with a 50 mm long measuring grid could be placed at a distance of one diameter from the edge of the core.

3) In the case of the one-way slabs, the measurement provided with less accurate instruments (such as easily accessible linear foil strain gauges) should be performed only in the longitudinal direction, as the stresses in transversal deflected directions are difficult to evaluate.

Acknowledgements

This paper was supported under the project of Operational Programme Integrated Infrastructure: Application of innovative technologies focused on the interaction of engineering constructions of transport infrastructure and the geological environment, ITMS2014+ code 313011BWS1. The project is co-funding by European Regional Development Fund.

References

[1] SUCHARDA, O. – MARCALIKOVA, Z. – GANDEL, R.: Microstructure, Shrinkage, and Mechanical Properties of Concrete with Fibers and Experiments of Reinforced Concrete Beams without Shear Reinforcement. Materials 2022, 15, 5707, https://doi.org/10.3390/ma15165707.
[2] HOLÝ, M. – ČÍTEK, D. – VRÁBLÍK, L.: The Experimental Timber–UHPC Composite Bridge. Sustainability, 2021, 13, 4895, https://doi.org/10.3390/su13094895.
[3] BUJŇÁKOVÁ, P.: Anchorage System in Old Post-tensioned Precast Bridges. Civil and Environmental Engineering, Vol. 16, Iss. 2, 2020, pp. 379-387, https://doi.org/10.2478/cee-2020-0038.
[4] DAOU, H. – RAPHAEL, W.: Ensemble Tree Machine Learning Models for Improvement of Eurocode 2 Creep Model Prediction. Civil and Environmental Engineering, Vol. 18, Iss. 1, 2022, pp. 174-184, https://doi.org/10.2478/cee-2022-0016.
[5] GALVÃO, N. – MATOS, J. C. – HAJDIN, R. – FERREIRA, L. – STEWART, M. G.: Impact of construction errors on the structural safety of a post-tensioned reinforced concrete bridge. Engineering Structures, Vol. 267, 2022, 114650, https://doi.org/10.1016/j.engstruct.2022.114650.
[6] DRUSA, M. – MIHALIK, J. – MUZIK, J. – GAGO, F. – STEFANIK, M. – RYBAK, J.: The Role of Geotechnical Monitoring at Design of Foundation Structures and their Verification – Part 2. Civil and Environmental Engineering, Vol. 17, Iss. 2, 2021, pp. 681-689, https://doi.org/10.2478/cee-2021-0067.
[7] BRACHACZEK, W. – CHLEBOŚ, A. – GIERGICZNY, Z.: Influence of Polymer Modifiers on Selected Properties and Microstructure of Cement Waterproofing Mortars. Materials 14, 2021, 7558, https://doi.org/10.3390/ma14247558.
[8] GAGO, F. – VALLETTA, A. – MUZIK, J.: Formulation of a Basic Constitutive Model for Fine - Grained Soils Using the Hypoplastic Framework. Civil and Environmental Engineering, Vol. 17, Iss. 2, 2021, pp. 450-455, https://doi.org/10.2478/cee-2021-0047.
[9] PARIVALLAL, S. – RAVISANKAR, K. – NAGAMANI, K. – KESAVAN, K.: Core-drilling technique for in-situ stress evaluation in concrete structures. Exp Tech, 35, 2011, pp. 29–34, https://doi.org/10.1111/j.1747-1567.2010.00622.x.
[10] ZANINI, M. A. – FALESCHINI, F. – PELLEGRINO, C.: New trends in assessing the prestress loss in post-tensioned concrete bridges. Front. Built Environ, 8, 2022, 956066, doi: 10.3389/fbuil.2022.956066.
[11] INNOCENZI, R. D. – NICOLETTI, V. – AREZZO, D. – CARBONARI, S. – GARA, F. – DEZI, L.: A Good Practice for the Proof Testing of Cable-Stayed Bridges. Appl. Sci. 12, 2022, 3547, https://doi.org/10.3390/app12073547.
[12] KRAĽOVANEC, J. – BAHLEDA, F. – PROKOP, J. – MORAVČÍK, M. – NESLUŠAN, M.: Verification of Actual Prestressing in Existing Pre-Tensioned Members. Appl. Sci. 11, 2021, 5971, https://doi.org/10.3390/app11135971.
[13] BAGGE, N. – NILIMAA, J. – ELFGREN, L.: In-situ Methods to Determine Residual Prestress Forces in Concrete Bridges. Eng. Struct. 135, 2017, pp. 41–52, https://doi.org/10.1016/j.engstruct.2016.12.059.
[14] MATHAR, J.: Determination of initial stresses by measuring the deformation around drilled holes. Transactions of ASME, Vol. 56, Iss. 4, 1934, pp. 249-254.
[15] DENG, N. C. – TANG, P. F.: Research on In Situ Stress Measurements in Reinforced Concrete Beams Based on the Core-Drilling Method. Advances in Civil Engineering, Vol. 2020, Article ID 8832614, 11 pages, 2020, https://doi.org/10.1155/2020/8832614.
[16] JOCH, R. – ŠAJGALÍK, M. – CZÁN, A. – HOLUBJÁK, J. – CEDZO, M. – ČEP, R.: Effects of Process Cutting Parameters on the Ti-6Al-4V Turning with Monolithic Driven Rotary Tool. Materials 15, 2022, 5181, https://doi.org/10.3390/ma15155181.
[17] CZÁN, A. – JOCH, R. – ŠAJGALÍK, M. – HOLUBJÁK, J. – HORÁK, A. – TIMKO, P. –

VALÍČEK, J. – KUŠNEROVÁ, M. – HARNIČÁROVÁ, M.: Experimental Study and Verification of New Monolithic Rotary Cutting Tool for an Active Driven Rotation Machining. Materials 15, 2022, 1630, https://doi.org/10.3390/ma15051630.

[18] FIB, Comité Euro – International du Béton: Strategies for Testing and Assessment of Concrete Structures. Guidance Report. fib Bulletin No. 243; 1998.

[19] TP 059: Assignment and Performing of Bridge Diagnostics. SSC Bratislava 2012. Available on: https://www.ssc.sk/files/documents/technicke-predpisy/tp/tp_059.pdf. In Slovak language.

[20] JGJ/T 384-2016: Technical Specification for Testing Concrete Strength with Drilled Core Method. JGJ/T 384-2016, China, 2016.

[21] KRAĽOVANEC, J. – PROKOP, J.: Indirect methods for determining the state of prestressing. Transportation Research Procedia, Vol. 55, 2021, pp. 1236-1243, https://doi.org/10.1016/j.trpro.2021.07.105.

[22] MCGINNIS, M. J. – PESSIKI, S.: Experimental Study of the Core-Drilling Method for Evaluating of In Situ Stresses in Concrete Structures. Journal of Materials in Civil Engineering, Vol. 28, Iss. 2, 2016, https://doi.org/10.1061/(ASCE)MT.1943-5533.0001294.

[23] MCGINNIS, M. J. – PESSIKI, S. – TURKER, H.: Application of Three-dimensional Digital Image Correlation to the Core-drilling Method. Experimental Mechanics, 45 (4), 2005, doi: 10.1007/BF02428166.

[24] MCGINNIS, M. J. – PESSIKI, S.: Experimental and Numerical Development of the Core-Drilling Method for the Nondestructive Evaluation of In-situ Stresses in Concrete Structures. 2006, ATLSS Reports, 05-05, https://preserve.lib.lehigh.edu/islandora/object/preserve%3Abp-4308206.

[25] AZIZINAMINI, A. – KEELER, B. J. – ROHDE, J. – MEHRABI, A. B.: Application of a New Nondestructive Evaluation Technique to a 25-Year-Old Prestressed Concrete Girder. PCI Journal, Vol. 41 (3), 1996, pp. 82-95.

[26] AGREDO CHÁVEZ, A. – GONZALEZ, J. – SAS, G. – ELFGREN, L. – BIANCHI, S. – BIONDINI, F. et al.: Available Tests to evaluate Residual Prestressing Forces in Concrete Bridges. IABSE Symposium Prague 2022, Challenges for Existing and Oncoming Structures - Report, International Association for Bridge and Structural Engineering, International Association for Bridge and Structural Engineering, 2022, pp. 1123-1131.

[27] TRAUTNER, C. – MCGINNIS, M. J. – PESSIKI, S.: Analytical and numerical development of the incremental core-drilling method of non-destructive determination of in-situ stresses in concrete structures. The Journal of Strain Analysis for Engineering Design, 45 (8), 2010, pp. 1-12, doi: 10.1243/03093247JSA600.

[28] ČERVENKA, V. – JENDELE, L. – ČERVENKA, J.: ATENA Program Documentation - Part 1. Theory, Červenka Consulting, Prague, Czech Republic, 2020, www.cervenka.cz/assets/files/atena-pdf/ATENA_Theory.pdf.

[29] ČERVENKA, J. – PROCHÁZKOVÁ, Z. – SAJDLOVÁ, T.: ATENA Program Documentation - Part 4-2. Tutorial for Program ATENA 3D, Červenka Consulting, Prague, Czech Republic, 28 September 2017, www.cervenka.cz/assets/files/atena-pdf/ATENA-Engineering-3D_Tutorial.pdf.

[30] ČERVENKA, V. – ČERVENKA, J.: ATENA Program Documentation - Part 2-2. User's Manual for ATENA 3D, Červenka Consulting, Prague, Czech Republic, November 2017, www.cervenka.cz/assets/files/atena-pdf/ATENA-Engineering-3D_Users_manual.pdf.